Microscopic description of ^{4}He $+$ ^{4}He elastic scattering over the energy range $E = 100$–280 MeV

M. El-Azab Farid

Physics Department, Assiut University, Assiut 71516, Egypt

Analysis of the differential cross sections for ^{4}He $+$ ^{4}He elastic scattering is performed within the framework of the double-folding optical model. Two appropriate effective nucleon-nucleon interactions are employed to generate the α-α folded real potentials. The obtained potentials in conjunction with phenomenological Woods-Saxon (WS) derivative imaginary potentials are used to investigate six sets of the elastic scattering data through the energy range 100–280 MeV. Successful reproduction of the data is obtained by both considered interactions. In addition, real phenomenological potentials expressed in a squared WS form are successfully used to reproduce these data.

I. INTRODUCTION

The fundamental importance to nuclear physics of the interaction between two α particles has long been recognized, and consequently, this interaction has been the subject of several theoretical [1–9] and experimental [10–19] studies. This importance arises from several characteristics of the $\alpha + \alpha$ system. (i) Such a relatively simple (few-nucleon) system provides the opportunity for carrying out fundamental calculations of the reaction. A number of calculations have been performed using the resonating-group method (RGM) to the $\alpha + \alpha$ system at c.m. energies below the reaction threshold of 17.36 MeV [2,9]. (ii) The spin and isospin saturation and high binding energy (28.3 MeV) of the α particle suggest that the α-particle-like substructures might be important constituents of light nuclei or of the surface region of heavy nuclei [20–26]. It was found that, for nucleon densities around one-third of that in the nuclear interior, condensation into α clusters is energetically favorable [27]. This was evidenced by α-transfer and α-knockout reactions [28]. Therefore, detailed knowledge of the $\alpha + \alpha$ interaction possibly could clarify certain aspects of the nuclear reaction mechanisms and nuclear structure. (iii) Besides the importance of the α-α interaction per se, the $\alpha + \alpha$ reaction is well known to play an important role in the nucleosynthesis of nature's elements [14,29–31]. At the sub-Coulomb energies characteristic of stellar interiors, the $\alpha + \alpha \rightarrow [^8\text{Be}]^*$ reaction provides the critical intermediate step in the 3α reaction, which leads to the formation of ^{12}C and heavier elements. At higher energies the $\alpha + \alpha$ collisions contribute significantly to the abundance of light elements (He, Li, Be, and B) via cosmic-ray-like processes.

Through the past four decades, measurements of elastic scattering differential cross sections for the reaction $^4\text{He}(\alpha, \alpha)^4\text{He}$ at different bombarding energies have been reported in several articles. Experimental and theoretical work on this system up to 1969 has been well reviewed in Ref. [32]. In 1976, measurements with large uncertainties over limited angular ranges ($\simeq 50°$–$100°$) were obtained at 650 and 850 MeV [12]. These data have been phenomenologically analyzed by Coker and Tamura [4]. Nadasen *et al.* [13] measured the elastic scattering differential cross sections at

158 MeV, which were also analyzed within the framework of a phenomenological optical potential. A few years later, poor elastic scattering data at 198 MeV were presented [14], but data with sufficient accuracy at the same energy were obtained by Cowley *et al.* [15]. In two sequence studies [17,18] new measurements of differential cross sections at 158 and 200 MeV were reported. Recently, Rao *et al.* [19] performed accurate measurements on $\alpha + \alpha$ elastic scattering at 280 and 620 MeV. These data are of interest because such data have not existed previously and because these data exhibit a systematic energy dependence when compared with measurements at lower energies.

In the light of this historical review, one may notice that phenomenological optical model (OM) analysis is the common tool for investigating all these elastic scattering data. The OM analysis using the conventional Woods-Saxon (WS) shape for the real and imaginary parts of the potential, although far from being fundamental, has presented the best means for the reproduction of the elastic scattering angular distributions, with six free parameters used in the data fits. However, it was pointed out [13,17,19] that an OM analysis with a six-parameter WS potential cannot reproduce the large-angle cross sections. Therefore, it was essential [13,17,19] to introduce a combination of two WS potentials for the real part in addition to a third one for the imaginary part, constituting a nine-parameter potential, to obtain successful predictions of the data. This combination of two different WS forms leads to a kink in the shape of the real potential. It was mentioned that the physical origin of this irregularity is not clear, so more theoretical investigation of the α-α interaction was recommended [19].

To our knowledge, despite the wide use of the double-folding (DF) model [33] to describe the α-nucleus scattering (e.g., Refs. [34–38] and references therein), no previous study has been reported to investigate $\alpha + \alpha$ elastic scattering differential cross section data within the framework of this approach. This lack of such research motivated us to perform the present work, which provides the first attempt to study six sets of these data covering a wide range of energies, namely, at incident energies of 100, 120, 140, 160, 200, and 280 MeV. The paper is organized in the following way.

In the next section the theoretical formalism is given. Numerical results and comparison to experimental data are presented and discussed in Sec. III. Finally, conclusions are summarized in Sec. IV.

II. THEORETICAL FORMALISM

The DF model has been extensively used to generate microscopically the real part of both α-nucleus and heavy-ion (HI) optical potentials, where an effective nucleon-nucleon (*NN*) interaction is folded with the mass distributions of both projectile and target nuclei. In the first order of Feshbach's theory for the optical potential, the projectile-target potential can be evaluated as a Hartree-Fock-type potential for the dinuclear system,

$$V = V_D + V_{EX} = \sum_{i \in A_P, j \in A_T} [\langle ij|\upsilon_D|ij\rangle + \langle ij|\upsilon_{EX}|ij\rangle], \quad (1)$$

where $|i\rangle$ and $|j\rangle$ refer to the single-particle wave functions of nucleons in the two colliding projectile (A_P) and target (A_T) nuclei and υ_D and υ_{EX} are, respectively, the direct and exchange parts of the chosen effective *NN* interaction.

The direct part is local, and by introducing one-body matrices of the α-particle density, with $\rho_\alpha(r, r) \equiv \rho_\alpha(r)$, one can explicitly deduce the α-α direct potential from the following double-convolution integral:

$$V_D(R) = \int \rho_\alpha(r_1)\rho_\alpha(r_2)\upsilon_D(\rho_\alpha, E, s)d\vec{r_1}\,d\vec{r_2},$$
$$s = |\vec{R} + \vec{r_2} - \vec{r_1}|. \quad (2)$$

The exchange potential V_{EX} is nonlocal and contains a self-consistency problem. The exact treatment of the nonlocal exchange term is complicated numerically, but one may obtain an equivalent local potential by using a realistic approximation for the mixed density matrix [36]. In the present work we confine our calculations to deduce the α-α direct potential.

The total α-α interaction may be written in the form

$$U(R) = -V(R) - iW(R) + V_C(R), \quad (3)$$

where the real part, $V(R)$, is obtained from the DF integral (2), and the imaginary part, $W(R)$, is treated phenomenologically by the surface WS form as

$$W(R) = [-4ia_iW_s(d/dR)]\left[1 + \exp\left(\frac{R - R_i}{a_i}\right)\right]^{-1}, \quad (4)$$

where W_s is the surface depth, $R_i = r_i \times 4^{1/3}$, and r_i and a_i are the radius and diffuseness parameters, respectively. $V_C(R)$ is the repulsive Coulomb interaction. The Coulomb potential is frequently represented by the interaction between two uniform charge distributions of radius equal to $1.3 \times 4^{1/3}$.

A. The nuclear density distribution

In general, the projectile and target matter densities are important ingredients in the DF model. In the present calculations we are concerned only with the α-particle density. Investigation of the nuclear matter density of the α particle in

detail is beyond the scope of this work. However, we briefly review appropriate forms previously used to represent the matter distribution in this nucleus.

The α-particle density can be computed from its wave function ψ_α, defined as [39]

$$\psi_\alpha = \exp\left[-\frac{a}{2}\sum_{i=1}^{4}\xi_i^2\right], \quad \sum_{i=1}^{4}\vec{\xi}_i = 0, \quad (5)$$

where $\vec{\xi}_i$ denote the position vectors of nucleons from the center of mass of the α particle. Then

$$\rho_\alpha(r) = \langle\psi_\alpha|\sum_{i=1}^{4}\delta(\vec{r} - \vec{\xi}_i)|\psi_\alpha\rangle/\langle\psi_\alpha|\psi_\alpha\rangle$$
$$= 4\left(\frac{\beta}{\pi}\right)^{3/2}\exp(-\beta r^2), \quad (6)$$

where $\beta = \frac{4}{3}a$. The root mean square (rms) radius of this density is given as

$$\langle r^2\rangle^{1/2} = \sqrt{\frac{1.5}{\beta}}. \quad (7)$$

This simple Gaussian shape was adopted for the α-particle density in numerous articles [11,33–45], where different values of the parameter β were suggested with rms radii ranging from 1.36 to 1.83 fm. However, there are two values of the nuclear rms radius for ^{4}He deduced from experimental measurements. One was obtained from elastic electron scattering (1.47 ± 0.02 fm) [46,47] and the other has been recently extracted from the analysis of the experimental interaction cross sections (1.58 ± 0.04 fm) using the Glauber model [48,49].

Despite the wide use of the Gaussian form (6), as the most convenient shape to represent the nuclear matter distribution in the α particle, some authors suggested different forms for this distribution. The two-parameter Fermi (2-pf) form

$$\rho_\alpha(r) = \rho_0 \Big/\left[1 + \exp\left(\frac{r - 1.5}{0.308}\right)\right] \quad (8)$$

was adopted by Warner *et al.* [50]. The obtained rms radius is 1.63 fm. The parameter ρ_0 can be extracted from the normalization condition

$$\pi \int \rho_\alpha(r)r^2 dr = 1. \quad (9)$$

In addition, Burov *et al.* [51] suggested the density form

$$\rho_\alpha(r) = 0.256\exp(-0.51r^2) + 0.029r^2\exp(-1.384r^2), \quad (10)$$

which yields a rms radius equal to 1.706 fm.

We tested these forms of the α-particle density in the folding calculations [52]. It was found that the form of Burov *et al.* [51] has the best ability to produce a successful description of the scattering data in the considered energy range. Therefore, in the present work, our DF calculations are confined only to this form [51].

B. Effective *NN* interactions

In the folding model the choice of the *NN* interaction is crucial. Several versions, including the JLM, M3Y, DDM3Y, BDM3Y, CDM3Y, S1Y, and KH effective *NN* interactions, have been used to fit the α-particle and HI elastic scattering angular distributions (e.g., Refs. [33–37,53–55]). To study the sensitivity of the results on the *NN* effective interaction, we have considered, in the present work, two examples. The first is a phenomenological single Yukawa term with a density independence and weak energy dependence, known as the S1Y interaction [53,55]. This interaction is defined as [53]

$$\upsilon(s) = \upsilon_0 \exp\left(-\frac{s}{\lambda}\right) \bigg/ \left(\frac{s}{\lambda}\right), \qquad (11)$$

where $\upsilon_0 \simeq 60(1 - 0.005E/A_P)$ MeV and the range $\lambda = 0.7$ fm. It was shown [53,55] that this interaction successfully describes peripheral HI elastic scattering at intermediate energies ($E/A_P \simeq 10$–85 MeV/nucleon), in which the strong absorption is dominated and the tail of the optical potential is relevant. Therefore, the use of this interaction in generating DF potentials for light HI systems, in which elastic scattering data are sensitive to the potential in the interior region at small radii, was avoided [53,56]. In the present work we test the validity of the S1Y effective interaction in analyzing the elastic scattering of a few-nucleon system. We use this interaction to deduce only the real part of the α-α DF optical potential; the imaginary part, as previously mentioned, is treated phenomenologically using the derivative WS form (4).

Because the density dependence of the *NN* interaction suggested by the Brueckner theory is very important for light HI scattering [57], as a second example, we have chosen the JLM effective *NN* interaction, which has a built-in target-density and energy dependence [58]. It has been parametrized [58] to be able to describe the nucleon-nucleus optical potential for energies up to 160 MeV and has been extended to be widely used [35,55] to generate the nucleus-nucleus potentials within the DF approach. The real part of the JLM effective *NN* interaction is expressed as

$$\upsilon_{\text{eff}} = h(s)\, V(\rho_\alpha, E), \qquad (12)$$

where

$$h(s) = \frac{1}{(t\sqrt{\pi})^3} \exp(-s^2/t^2). \qquad (13)$$

The range parameter t is chosen to equal 1.2 fm. Derivation details of the potential $V(\rho_\alpha, E)$ are given elsewhere [55,58].

We recall that both S1Y and JLM interactions are appropriate effective *NN* interactions for the energy range (25–70 MeV/nucleon) belonging to the α-α elastic scattering data considered in our study.

C. Phenomenological potentials

As mentioned in the introduction, it was reported in several articles [13–19] that the WS potential failed to reproduce the large-angle data. Therefore, to obtain satisfactory fits to these data, a combination of two WS potentials was used for the real central part of the interaction to provide more flexibility to the shape of the potential.

In the present work, we analyze the considered sets of data, also, using complex phenomenological potentials. We consider, however, the real part of the α-α interaction represented by only a single potential expressed in a squared WS form as

$$V(R) = V_0 \bigg/ \left[1 + \exp\left(\frac{R - R_0}{a_0}\right)\right]^2. \qquad (14)$$

The imaginary part, $W(R)$, as used with the real DF potentials, is given by the surface WS form (4).

III. PROCEDURE

Elastic scattering calculations are carried out using the computer code HIOPTM-94 [59]. The code is modified [60] to antisymmetrize the two identical bosons, resulting in only even partial waves in the partial wave decomposition of the scattering amplitudes. The inputs of mass and energies are taken as given by the relativistically corrected kinematics [61]. For instance, the relativistic enhancement in the reduced mass at an energy of 280 MeV is 0.0188%. Since for any identical-particles reaction no relativistic change exists in the c.m. momentum, therefore, this energy is corrected to be 274.838 MeV.

Best fits are obtained by minimizing χ^2, where

$$\chi^2 = \frac{1}{N} \sum_{k=1}^{N} \left[\frac{\sigma_{\text{th}}(\theta_k) - \sigma_{\text{ex}}(\theta_k)}{\Delta\sigma_{\text{ex}}(\theta_k)}\right]^2, \qquad (15)$$

$\sigma_{\text{th}}(\sigma_{\text{ex}})$ is the theoretical (experimental) cross section at angle θ_k in the c.m. system, $\Delta\sigma_{\text{ex}}$ is the experimental error, and N is the number of data points. An average value of 10% is used for the experimental errors of all considered data. Searches are carried out on four parameters: the real depth, υ_0 (for S1Y interaction), or renormalization factor, N_R (for JLM interaction), in addition to the WS form parameters (W_s, r_i, a_i). Searches on six free parameters are performed for the complex phenomenological potential analysis. For all considered potentials, the calculated differential elastic scattering cross sections are normalized by the factors 1.5, 1.13, 1.06, and 0.65 at energies of 100, 120, 200, and 280 MeV, respectively, while no normalization is used at the other energies.

IV. RESULTS AND DISCUSSION

The theoretical predictions of the angular distribution of differential cross sections deduced using the adopted complex phenomenological optical potentials defined by Eqs. (14) and (4) are shown in comparison with the experimental data in Fig. 1. The corresponding extracted best-fit parameters are listed in Table I. Obviously, for the six considered energies, the data are successfully reproduced over all the angular ranges using one-term phenomenological real potentials expressed by the squared WS form (14). These potentials are consistent in depth with those extracted in previous studies [13–19]. The imaginary surface potentials, as shown in Table I, are shallow and their depths, in general, decrease as energy increases.
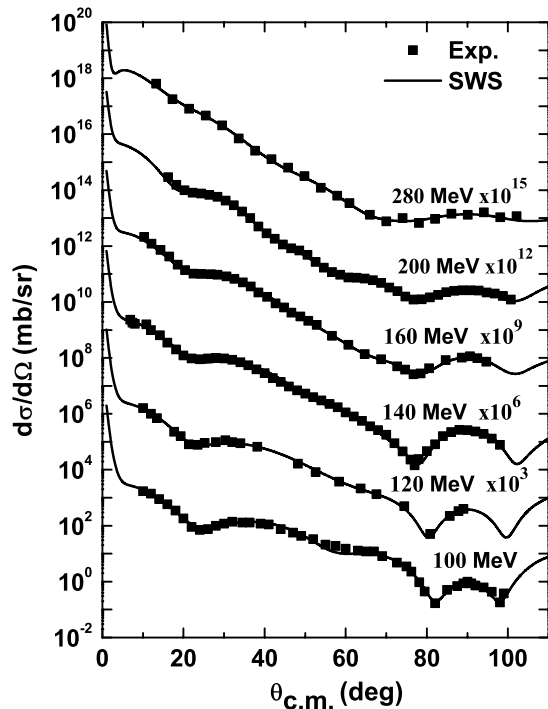
FIG. 1. Angular distributions of the ^{4}He + ^{4}He elastic scattering data in comparison with the OM results given by the phenomenological squared WS potentials.
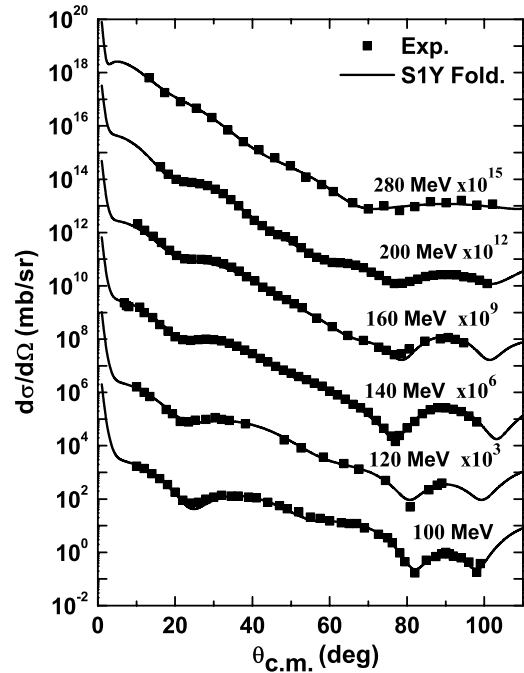

FIG. 2. The same angular distributions as in Fig. 1, but using DF potentials generated based upon the S1Y effective *NN* interaction.

In contrast, the DF optical model (2) based upon the S1Y interaction is performed to deduce the α-α potentials using the matter density distribution of Burov *et al.* [51]. The derived potentials, supplemented by imaginary surface WS potentials, are used to deduce the angular distributions of the $\alpha + \alpha$ elastic scattering cross sections, which are shown in Fig. 2. The best-fit parameters are listed in Table II. Figure 2 reveals that the DF potentials based upon the density-independent S1Y effective *NN* interaction produce satisfactory fits to the data over the entire measured angular range for the six considered energies. It is worth mentioning that searches on an imaginary volume WS potential in conjunction with the surface one result in acceptable fits at near zero depths of the volume part. This contrasts with the results obtained from analyses using phenomenological double WS potentials [13,17,19], where volume WS forms were required.

It is evident from Table II that the real strength (υ_0) clearly decreases as energy increases. As shown in Fig. 3, one can approximate this distribution by a linear energy dependence

relation as

$$\upsilon_0^{\alpha\text{-}\alpha}(E) = 122 - 0.72\,(E/A_P). \qquad (16)$$

This energy dependence reveals that the S1Y effective interaction required for the analysis of $\alpha + \alpha$ elastic scattering has a substantial stronger strength and decreases rapidly more than that adopted [53] for the analysis of HI scattering using the relation

$$\upsilon_0^{\text{HI}}(E) = 60 - 0.3\,(E/A_P). \qquad (17)$$

For α-α scattering, Eq. (16) implies that the real potential becomes repulsive beyond 170 MeV/n, whereas Eq. (17) indicates that a HI potential changes its sign beyond 200 MeV/nucleon. The DF potential based on the M3Y effective interaction changes its sign at 300 MeV/n. Rao *et al.* [19] deduced, recently, using the phenomenological OM analysis that the α-α interaction becomes repulsive beyond 1000 MeV/n, which is very high with respect to results of other interactions.

The DF calculations are also carried out to generate the real α-α potentials using the density- and energy-dependent JLM effective *NN* interaction and the density distribution of

TABLE I. Phenomenological optical potential parameters obtained by fits of the α-α scattering data.

Energy (MeV)	V_0 (MeV)	r_0 (fm)	a_0 (fm)	W_s (MeV)	r_i (fm)	a_i (fm)	J_R (MeV fm^3)	J_I (MeV fm^3)	χ^2	σ_R (mb)
100	171.1	1.340	1.307	30.3	1.975	0.122	483.2	114.4	2.69	383
120	147.3	1.459	1.178	18.5	1.669	0.326	452.6	139.3	1.15	419
140	115.1	1.610	1.016	20.9	1.654	0.291	406.0	137.1	2.55	380
160	174.5	1.207	1.280	11.8	1.574	0.462	394.8	118.7	1.25	382
200	135.9	1.498	1.101	15.0	1.627	0.516	421.7	183.0	1.52	464
280	151.2	1.061	1.240	6.1	0.901	0.189	260.8	7.9	2.00	33

TABLE II. Optical potential parameters used in the folding analysis of the α-α scattering data. The folding potentials are obtained using the S1Y effective NN interaction.

Energy (MeV)	v_0 (MeV)	W_s (MeV)	r_i (fm)	a_i (fm)	J_R (MeV fm^3)	J_I (MeV fm^3)	χ^2	σ_R (mb)
100	104.2	23.72	1.999	0.151	453.7	114.2	2.88	387
120	99.9	19.28	1.713	0.285	435.2	138.3	4.79	400
140	92.9	12.90	1.748	0.377	404.8	124.9	1.81	404
160	93.1	17.91	1.379	0.452	405.7	139.1	3.62	386
200	96.0	13.58	1.584	0.542	418.3	168.2	1.01	450
280	67.7	4.77	0.899	0.152	294.7	4.8	2.54	21

Burov *et al.* [51]. Cross-section calculations are performed by searching on four free parameters, a real renormalization factor N_R besides the imaginary WS parameters. The obtained best-fit parameters are listed in Table III and the corresponding predictions for the α-α elastic scattering differential cross sections are shown in Fig. 4 compared with the experimental data at the six considered energies.

As shown in Fig. 4, a successful description of the data is obtained over the entire measured angular ranges. This significant agreement between calculated and observed cross sections indicates that introducing an additional projectile-density dependence treatment is not required in the DF calculations to improve the fits with data. This conclusion may be confirmed since the best-fit renormalization factors N_R (see Table III) have almost negligible deviations ($\leqslant 0.03$) from unity. In several previous studies [22,35,62], it was pointed out that introducing reducing renormalization factors ($N_R \simeq 0.6$–0.7) is essential for the α-nucleus DF potentials to successfully reproduce elastic scattering data. Therefore, a projectile-density dependence factor was adopted. Also, Khoa [36] used slightly enlarging renormalization factors ($N_R > 1$) in the analysis of α-nucleus scattering through the energy range 100–173 MeV using DF potentials

based upon a realistic density-dependent M3Y (CDM3Y6) interaction.

Figure 5 shows the α-α potential at 120 MeV represented by different forms, where the phenomenological double WS forms of Refs. [16,17] (solid line) is compared with our squared WS (dashed line), S1Y (dotted line), and JLM (dot-dashed line) potentials. Similar results are obtained at other considered energies. Obviously, the compatibility between our phenomenological and folded potentials clearly dominates through the radial range $R > 1$ fm, whereas the agreement between the double WS potential [16,17] and our potentials starts at a wider radius, $R \sim 2.5$ fm. It is shown that the kink in the double WS potential spreads over the range $R > 1$–2.5 fm

In Fig. 6, a comparison is illustrated between real and imaginary volume integrals and reaction cross sections deduced from considered phenomenological and DF potentials. The energy dependence of the real volume integrals per nucleon
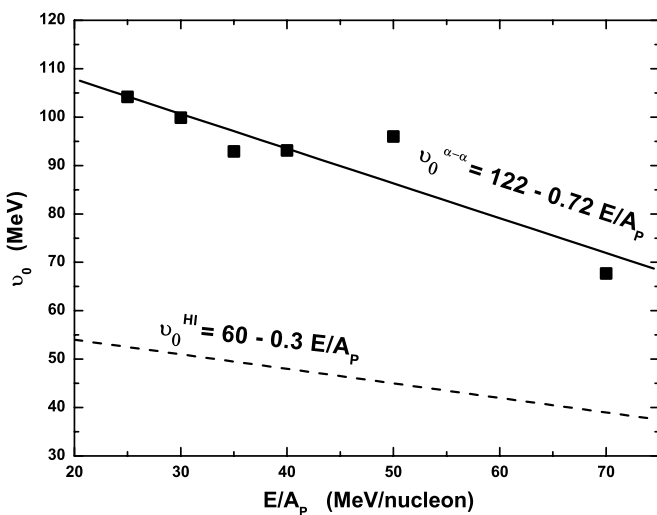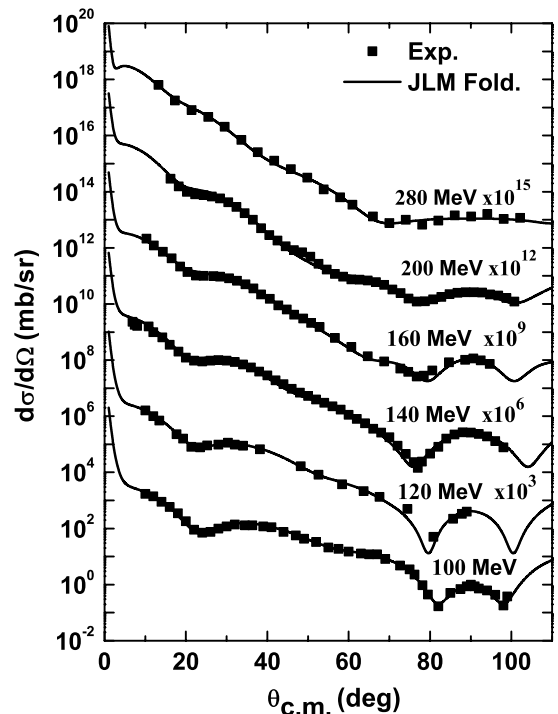

FIG. 3. Strength of the real S1Y effective interaction vs energy per incident nucleon. The straight line is the least-squares fit to the results. The relation deduced from analysis of HI scattering [53] is also shown.

FIG. 4. The same angular distributions as in Fig. 1, but using DF potentials generated based upon the JLM effective NN interaction.

TABLE III. Optical potential parameters used in the folding analysis of the α-α scattering data. The folding potentials are obtained using the JLM effective *NN* interaction.

Energy (MeV)	N_R	W_s (MeV)	r_i (fm)	a_i (fm)	J_R (MeV fm^3)	J_I (MeV fm^3)	χ^2	σ_R (mb)
100	1.00	18.11	1.949	0.210	475.6	115.9	1.52	415
120	1.03	20.95	1.786	0.269	467.1	146.3	2.10	400
140	0.97	9.32	1.850	0.472	417.8	129.4	5.56	401
160	0.97	12.47	1.457	0.461	397.5	109.0	3.28	359
200	1.03	8.75	1.733	0.507	385.3	117.0	4.37	378
280	1.03	5.27	0.842	0.191	314.4	6.0	3.32	26

pair is illustrated in the bottom of Fig. 5. The three considered potentials yield qualitatively and quantitatively consistent results. The general behavior of the energy dependence of the real volume integral J_R can be simulated by a linear relation as

$$J_R = J_0 - k E, \tag{18}$$

where $J_0 = 584$, 533, and 556 MeV fm^3 and $k = 1.086$, 0.78, and 0.88 fm^3 for the phenomenological, S1Y, and JLM potentials, respectively. We recall that the energy dependence of the real volume integral of the S1Y potential is related to that of the depth v_0, Eq. (16), where $J_R = 4.31 v_0$. In addition, the obtained energy coefficient (slope) k for the S1Y potential is in excellent agreement with those reported in Ref. [13] (0.65 ± 0.15 fm^3) and Ref. [17] (0.7 ± 0.08 fm^3).

The result of the JLM potential is slightly higher than those values.

The imaginary volume integrals, J_I, and total reaction cross sections, σ_R, obtained from the derived potentials are also shown, respectively, in the middle and top of Fig. 5. It is evident that the three considered potentials produce almost identical results, except that of the JLM potential at 160 MeV. We note also that, through the energy range 100–200 MeV, the J_I and σ_R values have no clear energy independence. This behavior of the imaginary volume integral is quite similar to that recently found by Rao *et al.* [19]. It is also obvious that the obtained reaction cross sections and the imaginary volume integrals have almost identical energy dependence. This result is physically expected where both J_I and σ_R concern the absorption to nonelastic channels.
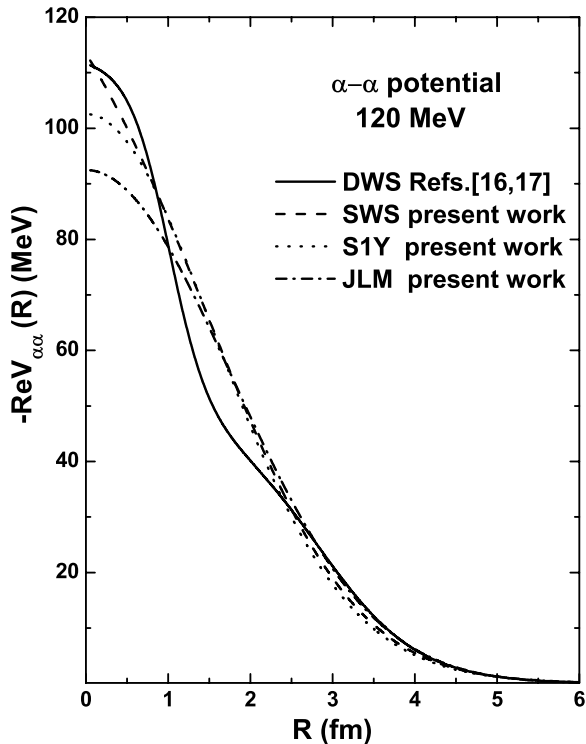

FIG. 5. The α-α potential at 120 MeV represented by phenomenological double WS forms of Refs. [16,17] (solid line) compared with our squared WS (dashed line), S1Y (dotted line), and JLM (dot-dashed line) potentials.
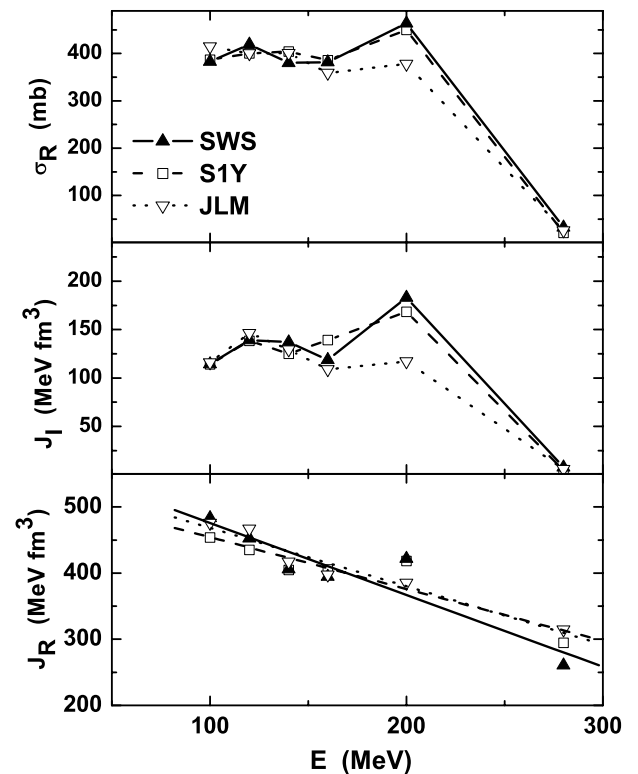

FIG. 6. Energy dependence of the real and imaginary volume integrals and reaction cross sections obtained by the phenomenological squared WS and DF potentials.

V. CONCLUSIONS

The present study has been devoted to analyze six sets of ^{4}He + ^{4}He elastic scattering data over the energy range 100–280 MeV within the framework of the OM. Three forms of the real α-α interaction are presented, while the imaginary part is kept fixed in a derivative WS form during the analysis using these real forms. First, phenomenological real potentials are parametrized in a single squared WS form. These potentials successfully reproduced the elastic scattering data over all the measured angular ranges. This is an interesting result, and it has been pointed out [13–19] that a combination of two WS forms is essential for providing successful predictions of the data, particularly at backward angles.

The double-folding model is employed to generate the real α-α interaction using two versions of the effective *NN* interactions, the phenomenological density-independent S1Y and a realistic density- and energy-dependent JLM. Although the S1Y effective interaction has been mainly proposed for the analysis of HI scattering at intermediate energies, our obtained DF potentials based upon this interaction have excellently reproduced the α + α scattering data at intermediate energies after modifying the strength and energy dependence rate (slope) adopted for HI scattering by a factor of about 2. Further, it is found that interaction strength has a linear energy dependence, with a slope significantly greater than that obtained from analysis of HI scattering, where the strength of the interaction vanishes at about 680 MeV.

The DF potentials based upon the JLM interaction also successfully reproduced the scattering data using renormal- ization factors very closed to unity ($\leqslant \pm 0.03$). This re- veals that, in contrast to results obtained from analysis of ^{6,7}Li scattering [55], modifying the JLM interaction by an additional projectile-density dependence approach, besides the built-in target-density treatment, in the α-α DF potentials is not apparently required.

The three investigated (WS and DF) potentials are evidently consistent with each other all over the radial range $R >$ 1 fm. In addition, the obtained real volume integrals from these potentials have a clear energy dependence, which is consistent with those previously deduced from phenomenological optical model analyses. Similar consistency is found for the imaginary volume integrals and reaction cross-section results.

Finally, it is worth concluding that the present study provides three forms of the real α-α potential to successfully reproduce the elastic scattering data at intermediate energies while having a realistic radial shape devoid of unphysical kinks, which were noticed [13,19] in the shape of the double WS phenomenological real potentials.

[1] S. Ali and A. R. Bodmer, Nucl. Phys. **80**, 99 (1966).

[2] V. G. Neudatchin, V. I. Kukulin, V. L. Korotkikh, and V. B. Korennoy, Phys. Lett. **B34**, 581 (1971).

[3] R. E. Brown and Y. C. Tang, Nucl. Phys. **A170**, 225 (1971).

[4] W. R. Coker and T. Tamura, Phys. Lett. **B62**, 374 (1976).

[5] B. Buck, H. Friedrich, and C. Wheatly, Nucl. Phys. **A275**, 246 (1977).

[6] A. I. Baz, V. Z. Goldberg, K. A. Gridnev, V. M. Semjonov, and E. F. Hefter, Z. Phys. A **280**, 171 (1977).

[7] L. Marquez, Phys. Rev. C **28**, 2525 (1983).

[8] G. Spitz, H. Klar, and E. W. Schmid, Z. Phys. A **322**, 49 (1985).

[9] S. A. Sofianos, H. Freideldey, R. Lipperheide, G. Pantis, and P. E. Hodgson, Nucl. Phys. **A540**, 199 (1992), and references therein.

[10] P. Darriulat, G. Igo, H. G. Pugh, and H. D. Holmgren, Phys. Rev. **137**, B315 (1965).

[11] W. S. Chein and R. E. Brown, Phys. Rev. C **10**, 1767 (1974).

[12] J. C. Fong *et al.*, Nucl. Phys. **A262**, 365 (1976).

[13] A. Nadasen *et al.*, Phys. Rev. C **18**, 2792 (1978).

[14] L. W. Woo, K. Kwaitkowski, S. H. Zhou, and V. E. Viola, Phys. Rev. C **32**, 706 (1985).

[15] A. A. Cowley, G. F. Steyn, S. V. Förtsch, J. J. Lawrie, J. V. Pilcher, F. D. Smit, and D. M. Whittal, Phys. Rev. C **50**, 2449 (1994).

[16] R. E. Warner, J. M. Fetter, R. A. Swartz, A. Okihana, T. Konishi, T. Yoshimura, P. D. Kunz, M. Fujiwara, K. Fukunaga, S. Kakigi, T. Hayashi, J. Kasagi, and N. Koori, Phys. Rev. C **49**, 1534 (1994).

[17] G. F. Steyn *et al.*, Phys. Rev. C **54**, 2485 (1996).

[18] G. F. Steyn *et al.*, Phys. Rev. C **57**, 1817 (1998).

[19] K. A. G. Rao, A. Nadasen, D. Sisan, W. Yuhasz, D. Mercer, S. M. Austin, P. G. Roos, and R. E. Warner, Phys. Rev. C **62**, 014607 (2000).

[20] F. Michel, Phys. Lett. **B60**, 229 (1976).

[21] M. El-Azab Farid, J. Phys. G **15**, 1437 (1989); **16**, 461 (1990).

[22] M. El-Azab Farid, Z. M. M. Mahmoud, and G. S. Hassan, Nucl. Phys. **A691**, 671 (2001); Phys. Rev. C **64**, 014310 (2001).

[23] M. El-Azab Farid, Phys. Rev. C **65**, 067303 (2002).

[24] P. E. Hodgson, Contemp. Phys. **31**, 99 (1990).

[25] H. Horiuchi, Eur. Phys. J. A **13**, 39 (2002).

[26] S. I. Fedotov, O. I. Kartavtsev, V. I. Kochkin, and A. V. Malykh, Phys. Rev. C **70**, 014006 (2004).

[27] D. Brink and J. J. Castro, Nucl. Phys. **A216**, 109 (1973).

[28] A. Nadasen *et al.*, Phys. Rev. C **39**, 536 (1989); A. Nadasen *et al.*, *ibid.* **47**, 674 (1993); A. Nadasen *et al.*, *ibid.* **59**, 760 (1999), and references therein.

[29] C. H. King, H. H. Rossner, S. M. Austin, W. S. Chein, G. J. Mathews, V. E. Viola, and R. G. Clark, Phys. Rev. Lett. **35**, 988 (1975).

[30] C. H. King, S. M. Austin, H. H. Rossner, and W. S. Chein, Phys. Rev. C **16**, 1712 (1977).

[31] B. G. Glagola, V. E. Viola Jr., H. Breuer, N. S. Chant, A. Nadasen, P. G. Roos, S. M. Austin, and G. J. Mathews, Phys. Rev. C **25**, 34 (1982).

[32] S. A. Afzal, A. Ahmad, and S. Ali, Rev. Mod. Phys. **41**, 247 (1969).

[33] G. R. Satchler and W. G. Love, Phys. Rep. **55**, 183 (1979).

[34] D. T. Khoa, G. R. Satchler, and W. von Oertzen, Phys. Rev. C **56**, 954 (1997).

[35] S. A. E. Khallaf, A. M. A. Amry, and S. R. Mokhtar, Phys. Rev. C **56**, 2093 (1997).

[36] D. T. Khoa, Phys. Rev. C **63**, 034007 (2001).

[37] M. Avrigeanu, W. von Oertzen, A. J. M. Plompen, and V. Avrigeanu, Nucl. Phys. **A723**, 104 (2003).

[38] M. M. Billah, M. N. A. Abdullah, S. K. Das, M. A. Uddin, A. K. Basak, I. Reichstein, H. M. Sen Gupta, and F. B. Malik, Nucl. Phys. **A762**, 50 (2005).

[39] R. M. De Vries, J. Perrenoud, I. Slaus, and J. W. Sunier, Nucl. Phys. **A178**, 424 (1972).

[40] I. Tanihata *et al.*, Phys. Lett. **B289**, 261 (1992).

[41] S. Funada, H. Kameyama, and Y. Sakuragi, Nucl. Phys. **A575**, 93 (1994).

[42] C. H. Dasso, J. L. Guisado, S. M. Lenzi, and A. Vitturi, Nucl. Phys. **A597**, 473 (1996).

[43] D. Baye, L. Desorgher, D. Guillain, and D. Herschkowitz, Phys. Rev. C **54**, 2563 (1996).

[44] V. B. Soubbotin and X. Vinas, J. Phys. G **25**, 2087 (1999); Nucl. Phys. **A665**, 291 (2000).

[45] G. D. Alkhazov *et al.*, Nucl. Phys. **A712**, 269 (2002).

[46] J. S. McCarthy, I. Sick, and R. R. Whitney, Phys. Rev. C **15**, 1396 (1977).

[47] H. De Vries, C. W. De Jager, and C. De Vries, At. Data Nucl. Data Tables **36**, 495 (1987).

[48] J. S. Al-Khalili, J. A. Tostevin, and I. J. Thompson, Phys. Rev. C **54**, 1843 (1996).

[49] O. M. Knyakzov, I. N. Kuchtina, and A. Fayans, Phys. Part. Nucl. **30**, 369 (1999).

[50] R. E. Warner *et al.*, Phys. Rev. C **54**, 1700 (1996).

[51] V. V. Burov, O. M. Knyazkov, A. A. Shirokova, and K. V. Shitikova, Z. Phys. A **313**, 319 (1983).

[52] M. El-Azab Farid (unpublished).

[53] G. R. Satchler, Nucl. Phys. **A579**, 241 (1994).

[54] M. El-Azab Farid and G. R. Satchler, Nucl. Phys. **A438**, 525 (1985); **A441**, 157 (1985).

[55] M. El-Azab Farid and M. A. Hassanain, Nucl. Phys. **A678**, 39 (2000); **A697**, 183 (2002); Eur. Phys. J. A **19**, 231 (2004).

[56] J. R. Beene, D. J. Horen, and G. R. Satchler, Phys. Lett. **B344**, 67 (1995); Nucl. Phys. **A596**, 137 (1996).

[57] D. T. Khoa, W. von Oertzen, and H. G. Bohlen, Phys. Rev. C **49**, 1652 (1995); D. T. Khoa, G. R. Satchler, and W. von Oertzen, *ibid.* **51**, 2069 (1995).

[58] J. P. Jeukenne, A. Lejeune, and C. Mahaux, Phys. Rev. C **16**, 80 (1977).

[59] N. M. Clarke (unpublished).

[60] M. El-Azab Farid (unpublished).

[61] M. El-Azab Farid and G. R. Satchler, Phys. Lett. **B146**, 389 (1984).

[62] F. Carstoiu and M. Lassaut, Nucl. Phys. **A597**, 269 (1996).